

Curie-Temperature Depth, Geothermal Gradient and Heat Flow Deduce from Spectral Analysis of Gravity Data of Chad Basin Northeast Nigeria

Sulaiman Garba Yana^{1,2}, Juzhi Deng^{1,2}, Hui Chen^{1,2}, Yanguo Wang^{1,2}

¹State Key Laboratory of Nuclear Resources and Environment, East China University of Technology, Nanchang, Jiangxi Province, China, 330013

²School of Geophysics and Measurement-control Technology, East China University of Technology, Nanchang Jiangxi Province, China, 330013

Corresponding author address: jzhdeng@ecut.edu.cn.

Abstract: *The purpose of the study is to estimate the curie-point depth, geothermal gradient, and heat flow in the Chad basin, which is deduced from spectral analysis of gravity data of Chad basin, Northeast Nigeria. The area is bounded by latitudes 9.50N – 11.00N and longitudes 9.50E - 12.50E in the Northeastern part of Nigeria. It covers a total land area of 230, 000km². The qualitative and quantitative interpretations of the Bouguer anomaly map were carried out using spectral analysis. The Bouguer gravity anomaly ranges from -55.5 to 26.4mgal with northeast to southwest trend. Therefore, the graben in the basin is connected with low heat flow and low negative Bouguer gravity anomaly. The study disclosed that a decrease in heat flow is noticed with an increasing sedimentary thickness. The result shows that the Curie point depths, range from 5.77km to 13km, with a mean value of 9.21km, geothermal gradient, range from 44.62 0C km⁻¹ to 107.210C km⁻¹, with a mean value of 75.92 0C km⁻¹ and heat flow, range from 111.55mWm⁻² to 268.03mWm⁻², with a mean value of 189.79mWm⁻². This result is excellent for utilization for exploration of an alternative source of geothermal energy. Therefore, the spectral depth analysis data in coexistence with heat flow information disclosed an almost linear relationship between heat flow and Curie-point depths.*

Keywords: Curie point depth, geothermal gradient, heat flow, gravity depth to basement, Chad basin

1. Introduction

The study was carried out to determine Curie Point Depth, Geothermal gradient, and Heat flow of the Chad basin, using gravity data. The data processing was accomplished, through the polynomial fitting, upward continuation, and spectral analysis to determine depth to centroid and depth to the top boundary and consequently the assessment of the curie isotherm, geothermal gradient, and heat flow.

The quest for the search for geothermal energy has been necessitated as a result of the over-dependence on the oil sector, neglecting other earth endowments. This has an adverse effect on the country in terms of a fall in oil prices. Diversifying economy to other sectors such as geothermal energy and mineral resources will increase the economic growth and hence better living for the citizenry. The project will serve as a lead for detailed geophysical surveys for economic prospects and well comprehension of the geology of the region in terms of sites for geothermal plants, which could be used for the generation of electricity, domestic, industrial, and agricultural purposes.

The findings of this study revealed that Curie Point Depth varies from 5.77km to 13.00km; Geothermal Gradient, 44.62⁰Ckm⁻¹ to 107.21⁰Ckm⁻¹, and Heat Flow, 111.55mWm⁻² to 268.03mWm⁻². These results are useful in understanding the variation in crustal thickness, thermal maturation of sediments and sites for geothermal energy.

Geophysical explorations are directed at acquiring indirectly, from the surface or from shallow depth, the physical parameters of the geothermal systems. A geothermal system is composed of four major elements: a heat source, a

reservoir, and a fluid, which is the transporter of that transfer of the heat, and a recharge area. The heat source is mostly a shallow magmatic body, normally cooling and frequently still partially molten. The volume of rocks from which heat can be removed is called the geothermal reservoir, which contains hot fluids, a summary term expressing hot water, vapour, and gases. A geothermal reservoir is ordinarily encircled by colder rocks that are hydraulically associated with the reservoir. Consequently, water may pass from colder rocks outside the reservoir (recharge) towards the reservoir, where hot fluids pass under the control of buoyancy forces towards a discharge area. Geothermal systems exist in areas of very high crustal heat flux that may be connected with the happening of young igneous bodies or hot rocks situated deeper in the crust [1], [2], [3].

Therefore, the use of gravity data to evaluate Curie's temperature-depth is not absolutely new and has been applied to many parts of the world, either by utilizing the frequency domain technique or analyzing isolated gravity anomalies due to discrete sources. The present research utilizes spectral analyses technique to evaluate Curie-temperature depth and heat flow to estimate the geothermal energy of the area.

On the other hand, the evaluation of change of the curie isotherm of an area can bestow valuable features about the regional temperature dispensation at depth and the concentration of beneath the surface geothermal energy [4]. Therefore, one paramount parameter that determines the relative depth of the curie isotherm with respect to sea level is the local thermal gradient i.e. heat flow [5]. The results have manifested that an area with outstanding geothermal energy is characterized by an anomalous high-temperature gradient and heat flow [4Tselentis, 1991]. It is therefore expected that

geothermally active regions would be related to shallow Curie point depth [6]. Estimates of depth to Curie temperature can grant valuable understanding in the evaluation of geothermal energy, estimation of thermal conductivity, and tectonic/geodynamic evolution. In this present research, we studied the geothermal structure of the Chad basin, based on the Curie point depth estimations. This project is emphasisfilling the missing gap in the crustal temperature information of the study area in addition to providing clues to possible productive areas. The results will throw more light on the geology and other features of the area, including the depth to gravity sources and curie-temperature depth.

2. Location and geology of the study area

The Chad Basin lies within a vast area of Central and West Africa at an elevation of between 200 and 500 m above sea level and covering 230,000km² (Figure 1). The basin has been referred to as an interior sag basin [7], due to a drooping incident that has pretentious it before the onset of continental segregation through which a rift system junction was set up providing a proper area for sedimentation. It, therefore, recline at the joint of basins (including the West African rift) which becomes effective in the Early

Cretaceous when Gondwana begin to break into section plates [8]. Stratigraphic interpretations of the Southern Chad Basin (Nigerian sector) are accessible in [8], [9], [10]. Sediments are mostly continental, rarely fossiliferous, imperfectly sorted, and middle-sized to coarse-grained, feldspathic sandstones called the Bima Sandstone. A transitional calcareous deposit-Gongila Formation that accompanied the onset of marine incursions within the basin overlies the Bima Sandstones. Therefore, these are overlain unconformably by graptolitic Keri-Keri Shales while the Chad Formation overlies it to the Earth's surface. [11] gives out a model for the regional structure and tectonic evolution of the Cretaceous Paleogene rift basins of Niger, Chad, and the Central African Republic. Both geophysical and geological clarification of data recommend a complex series of Cretaceous grabens straighten from the Benue Trough to the southwest. These data hinted related tectonic genesis entailing crustal thinning inside and underneath the grabens and the near-surface presence of igneous intrusions inside the horst/graben framework overlain by a fairly thick sequence of sedimentary materials. Figure 2 below shows the geology map of the study area.

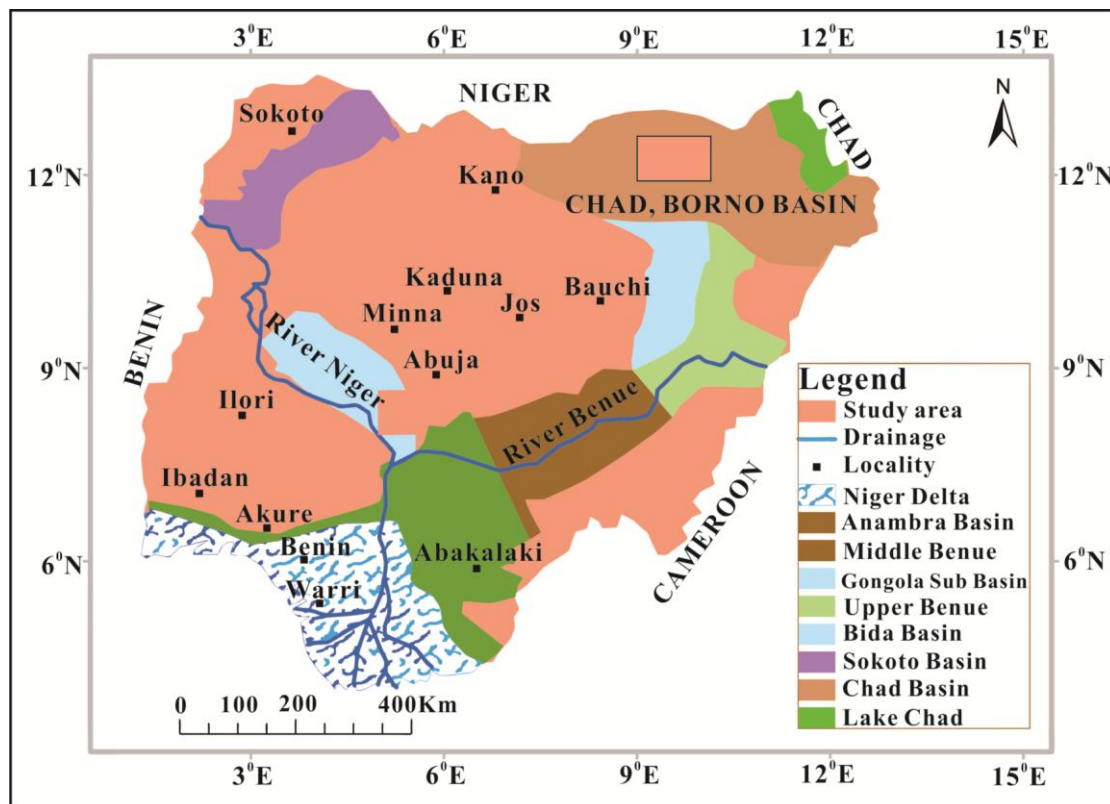


Figure 1: Geologic map of Nigeria showing the Chad Basin [12]

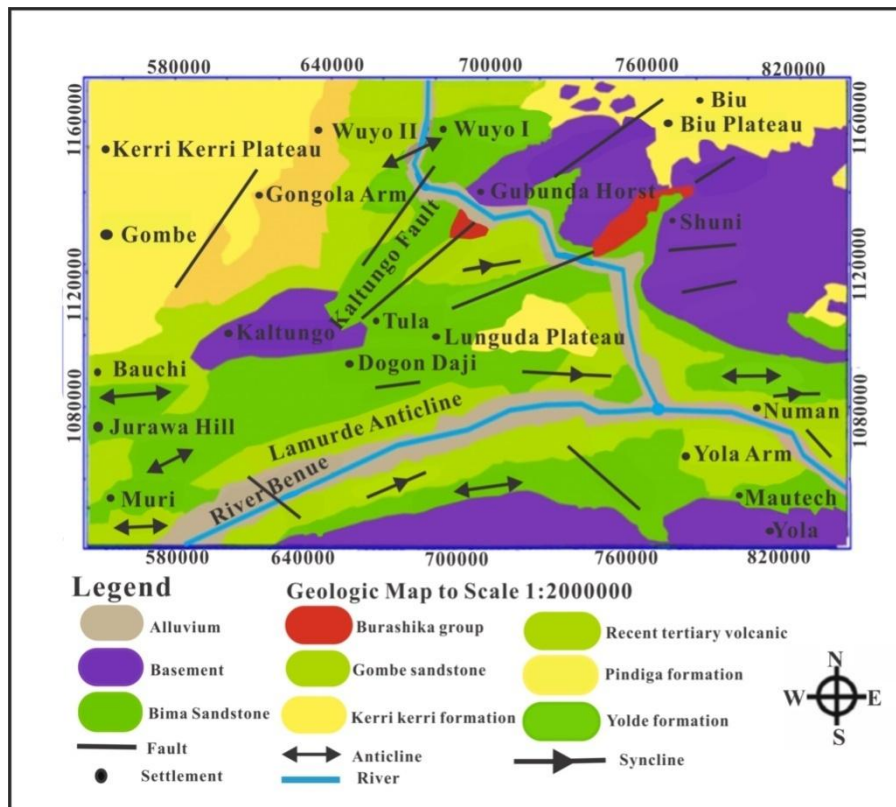


Figure 2: Geologic map of the study area. [13]

3. Materials and methods

The gravity data utilized for this research was modified from Cratchley as cited by [14]. The data were acquired with the help of a Worden prospecting gravity meter. The Bouguer gravity anomaly map is shown in Figure 3. A qualitative clarification of the gravity map was performed for the study area, and outcomes were compared with heat flow and depth to the basement of the study area.

The processing of the gravity data was carried out using various filters that will reveal certain features that will aid the interpretation. Thus the digital data was imported into the computer to produce the Bouguer gravity anomaly map. The Bouguer gravity anomaly map was further subjected to high-resolution filtering techniques such as polynomial fitting to obtain the regional and the residual maps, upward continuation, Spectral analysis, Curie point depths, geothermal gradient, and heat flow. Therefore, all these were carried out using the Oasis montaj software 8.0.

The Polynomial fitting procedure was utilized in regional-residual separation to acquire the residual map. In polynomial fitting, the regional is matched with mathematical Polynomial of low order to reveal the residual characteristic as random errors, and the analysis is based on statistical hypothesis. The observed data are used to compute, usually by the least square method, the mathematically described surface given the closest fit to the gravity field that can be obtained within a specified degree of detail. This surface is considered to be the regional field and the residual is the difference between the gravity field values thus determined [15]. The easiest approach is to fit a polynomial of the first order to the gravity data over a huge region as possible around the area of interest and to subtract the polynomial surface

from the observed surface. If the regional field were a simple inclined plane it will be a first-order surface. Thus

$$Z = A_x + B_x + C \quad (1)$$

The next stage of complexity is the representation of a second order polynomial where,

$$Z = Ax^2 + By^2 + CxyDx + F \quad (2)$$

The next stage of complexity is another representation of a third order polynomial, etc.

The residual gravity field of the study area was produced by subtracting the regional field from the Bouguer gravity field using the Polynomial fitting method. The computer program aero-super map was used to generate the coordinates of the gravity field data values. This super data file, for all the gravity values, was used for the production of the Bouguer anomaly map of the study area using Oasis Montaj software version 8.0. The program was used to derive the residual gravity values by subtracting values of the regional field from the Bouguer gravity field values (Figure 3) to produce the residual gravity map (Figure 4).

The upward continuation was used in order to simplify the appearance of regional gravity anomalies by suppressing the effects due to local features. The proliferation of local gravity anomalies often obscures the regional features. Upward continuation thus smoothed out these disturbances without impairing the main regional features. The main purpose of upward continuation is to view the gravity field density at a height above flight level so as to eliminate short-wavelength anomalies by emphasizing longer ones reflecting regional features. The equation of upward continuation is given by [16] as;

$$F(x, y, -h) = \frac{h}{2\pi} \iint \frac{f(x, y, 0) \partial x \partial y}{(x-x')^2 + (y-y')^2 + h^2}^{1/2} \quad (3)$$

Where $F(x', y', -h)$ = total field at a point $F(x', y', -h)$ above the surface on which $F(x', y', -0)$ is known h = continuation height.

This function decays steadily with increasing wavenumber, attenuating the higher wavenumber associated with such features and enhances, relatively the anomalies of the deep-seated sources because this form continuation successfully polished the anomaly, by repressing the short wavelength components. For this study upward continuation was carried out to eliminate local gravity sources so that the regional sources are enhanced for Curie point-depths calculations. The data was upward continued to 5km (Figure 5). The upward continued data was subjected to spectral analysis, to achieve that the data set was divided into a block of 18 data points, measuring about 15" x 15" which is equal to 27km x 27km from where the curie point was estimated using Oasis Motaj and Matlab software.

Curie point depth was estimated in two steps [17],[18]: to perform the analysis the first step was to estimate the depth to the centroid (Z_0) of the gravity source from the slope of the longest part of the wave length spectrum.

$$\ln \left[\frac{p(s)^{1/2}}{s} \right] = \ln A - 2\pi / s / Z_0 \quad (4)$$

Where $p(s)$ is the radially averaged power spectrum of the anomaly, s is the wavenumber and A is a constant.

The second step was the estimation of the depth to the top boundary (Z_t) of that distribution from the slope of the second-longest wavelength spectral segment [18].

$$\ln p(s)^{1/2} = \ln B - 2\pi / s / Z_t \quad (5)$$

Where B is the sum of the constant, the basal depth independent of s . Then the basal depth (Z_b) of the gravity source was calculated using the equation below.

$$Z_b = 2Z_0 - Z_t \quad (6)$$

The basal depth Z_b of the gravity source in the area is assumed to be the Curie point depth [16],[17].

Heat flow is the transfer of heat (energy) from the inner part of the earth to the surface. Therefore, the source of the majority of heat derives from the cooling of the earth's core and the radioactive heat-producing in the upper 20 to 40 km of the earth's crust. An average Curie point temperature of 580°C for crustal rocks is recommended [19],[20].

The estimation of heat flow and the thermal gradient was calculated using the Fourier's Law with the following formula

$$q = \lambda \left[\frac{\partial T}{\partial Z} \right] \quad (7)$$

Where q is the heat flow and λ is the coefficient of thermal conductivity. In this equation, it was assumed that the direction of the temperature variation is vertical and the temperature gradient $\left[\frac{\partial T}{\partial Z} \right] = \frac{\theta}{Z_b}$ is constant. According to [21], the Curie temperature (θ) is obtained from the Curie point depth (Z_b).

$$\theta = \left[\frac{\partial T}{\partial Z_b} \right] \quad (8)$$

Provided that there are no heat sources or heat sinks between the earth's surface and the Curie point depth, the surface temperature is 0°C and $\left[\frac{\partial T}{\partial Z} \right]$ is constant. The Curie temperature depends on the magnetic mineralogy. From equation 7 and equation 8 a relationship was determined between curie depth (Z_b) and the heat flow q , using the following formulae.

$$q = \lambda \left[\frac{\theta}{Z_b} \right] \quad (9)$$

Moreover from the above equation the Curie-point depth is inversely proportional to the heat flow [21], [22]. The geothermal gradient was calculated using equation 8 and a Curie point temperature of 580°C. Furthermore, the heat flow (q) of the region was determined using equation 9. In calculating temperature distribution in the crust, thermal conductivity (λ) is assumed to have a constant value in the range of 2 to 4 $\text{Wm}^{-1}\text{C}^{-1}$ [23]. In this study, the thermal conductivity (λ) of 2.5 $\text{Wm}^{-1}\text{C}^{-1}$ as the average for igneous rocks was used [21], [20Nwanko, 2007], [23], [24].

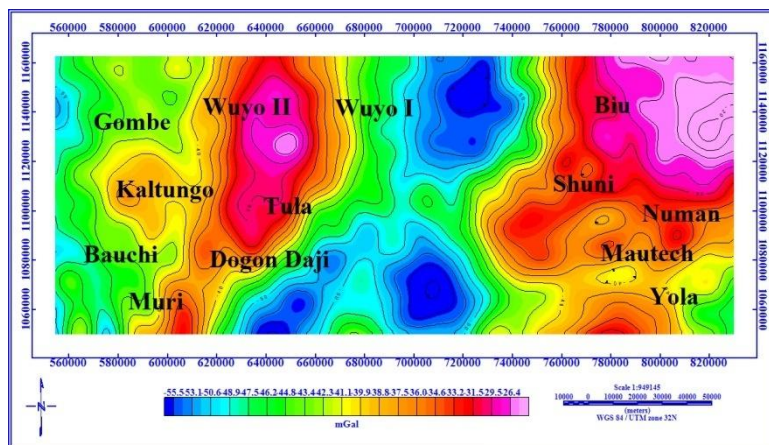


Figure 3: Bouguer anomaly map of the study area.

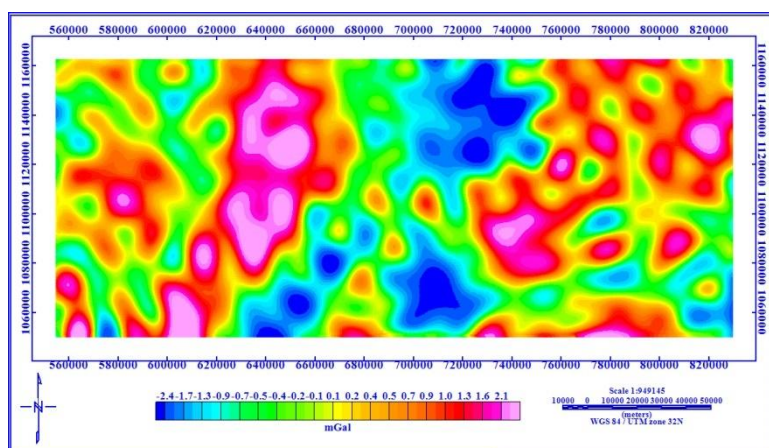


Figure 4: Residual of Upward continuation of gravity grid to 3000m altitude

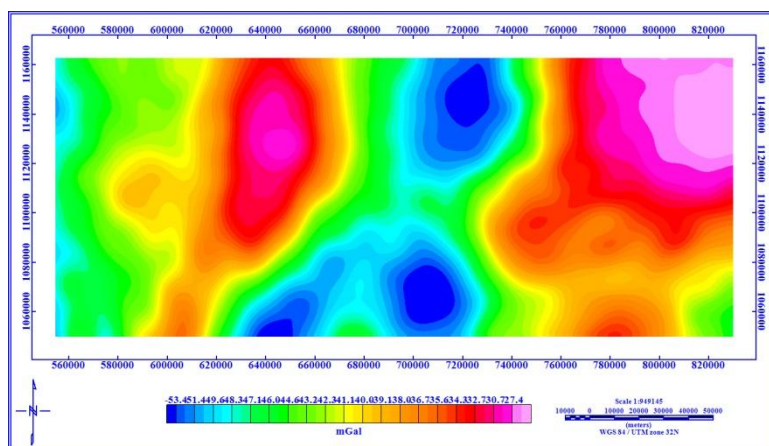
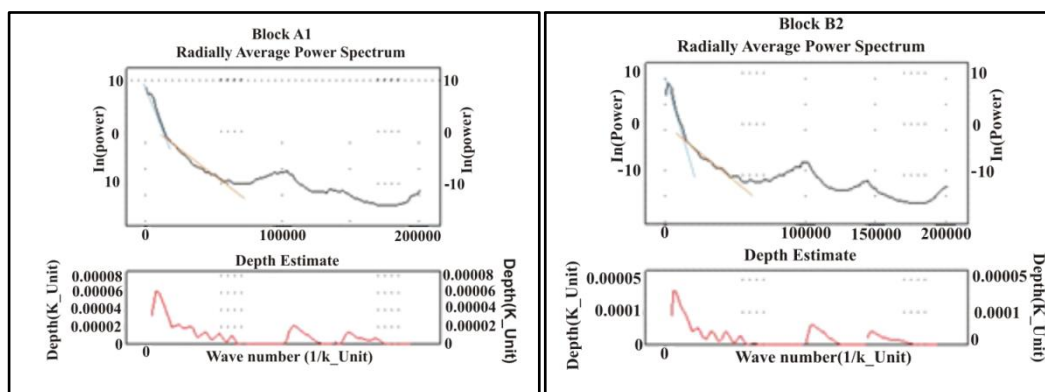


Figure 5: Upward Continuation Map of the Gravity data of the study area @3000m.



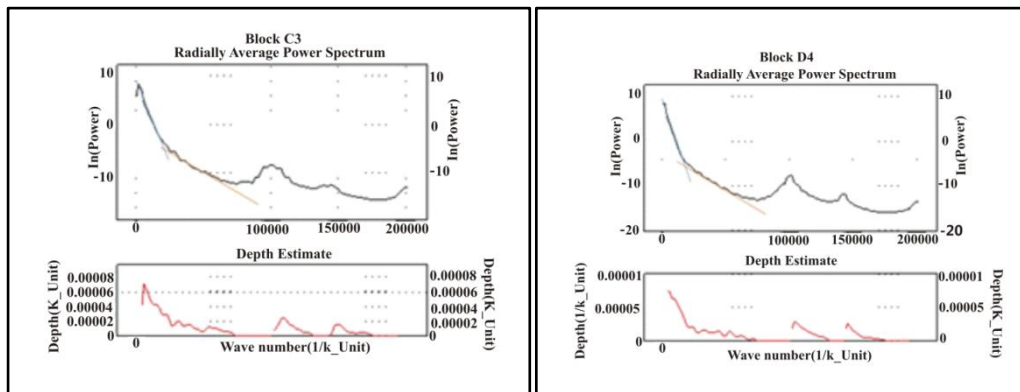


Figure 6: Radially Averaged Power for the 18 Spectral block cells (block A₁ to D₄) for Estimation of Depth to the bottom of gravity source using spectral analysis. But only 4 spectral block cells were displayed here for reference purpose.

Table 1: Calculated Curie depth, geothermal gradient and heat flow of gravity data

Block ID	Longitude (m)	Latitude (m)	Deep depth (Z_0)	Shallow depth (Z_t)	Curie depth (Z_b) $Z_b = 2Z_0 - Z_t$	Geothermal gradient $\left(\frac{dT}{dz}\right) ^\circ\text{CKm}^{-1}$	Heat flow (q) mWm^{-2}
A1	553705.7	1103241	6.20	1.70	10.70	54.21	135.53
B2	599742	1103339	5.00	1.95	8.05	72.05	180.13
C3	645783.3	1103495	4.80	1.28	8.32	69.71	174.28
D4	691832.1	1103709	6.20	1.78	10.62	54.61	136.53
E5	737890.6	1103982	4.70	2.07	7.33	79.13	197.83
F6	783961.2	1104314	3.60	1.43	5.77	100.52	251.30
G7	553725.3	1089973	4.40	1.30	7.50	77.33	193.33
H8	599778.3	1090069	3.55	1.29	5.81	99.83	249.58
I9	645836.4	1090224	7.50	2.00	13.00	44.62	111.55
J10	691902	1090436	4.30	1.49	7.11	81.58	203.95
L11	737977.3	1090706	3.60	1.22	5.98	96.99	242.48
M12	784064.7	1091034	4.80	1.38	8.22	70.56	176.40
N13	553743	1077811	3.85	1.08	6.62	87.61	219.03
O14	599811.2	1077906	4.80	1.38	8.22	70.56	176.40
P15	645884.5	1078059	3.70	1.39	6.01	96.51	241.28
Q16	691965.3	1078268	4.20	1.50	6.90	84.06	210.15
R17	738055.8	1078536	3.60	1.79	5.41	107.21	268.03
S18	784158.5	1078860	3.75	1.38	6.12	94.77	236.93
Average			5.53	1.58	9.21	75.92	189.79

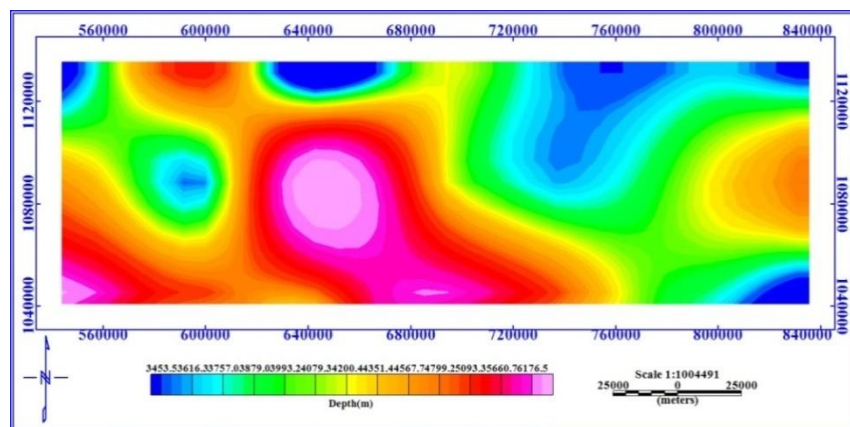


Figure 7: Deep depth to Gravity basement Map of the study area

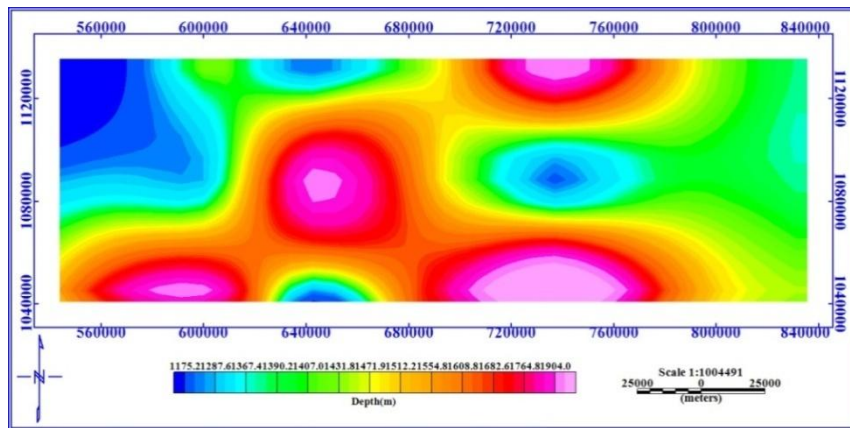


Figure 8: Shallow depth to gravity basement Map of the study area

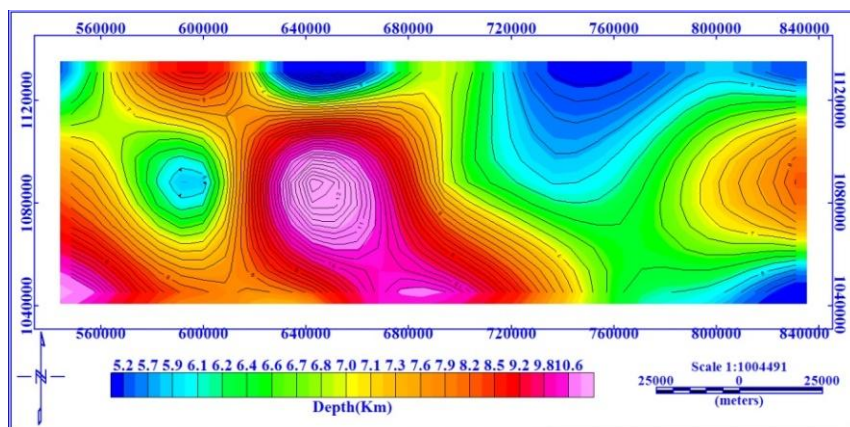


Figure 9: Gravity curie depth contour map of the study area (Km)

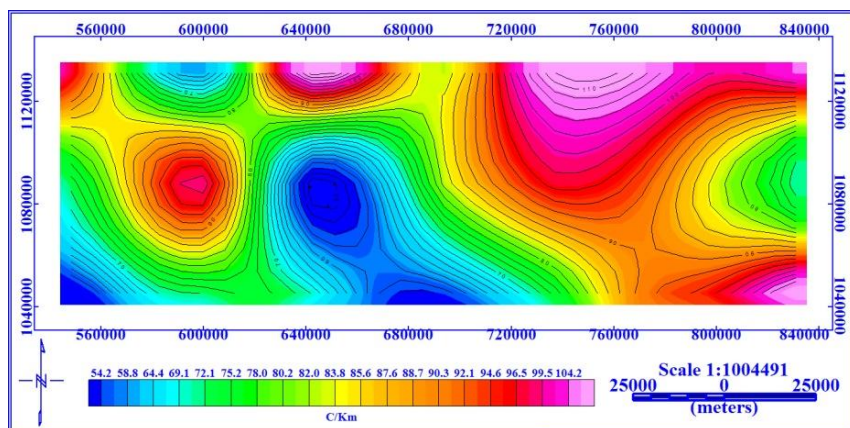


Figure 10: Gravity geothermal gradient contour map of the study area ($^{\circ}\text{CKm}^{-1}$)

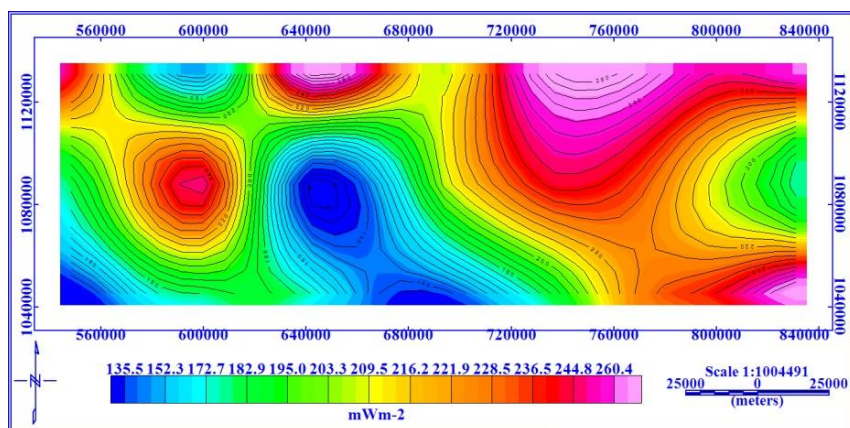


Figure 11: Gravity heat flow contour map of the study area (mWm^{-2})

4. Results and Discussion

A Bouguer anomaly map of the study area was thus prepared to interpret the study area's crustal structure (Figure 3). The grid map disclosed big-scale negative Bouguer anomalies trending Southwest-northeast to east-west over the central part of the study area. Closer geological and structural observation of this anomaly's axes suggested that its general trend followed an inferred granite intrusion area known as porphyritic granite. The quite different nature of the Bouguer gravity map on the eastern and western side was marked by gravity highs, bounded by relatively steep gradients occurring over or near high metamorphic formation (granulites, migmatites, and mica-schist) and other granitic plutons, suggesting the existence of a suture zone between two of the crust's blocks [25]. Hence, a positive Bouguer gravity anomaly in the southern region trending southwest-northeast manifested the intrusion of dense rocks (charnockites) in this area. The appearance of linear patterns and prominent steep gradients on previous locations may be suggesting the existence of major basement fault lines. The close negative anomaly may be connected to sedimentary basins and/or grabens.

Descriptions of gravity and magnetic data can be assisted by employing advanced processing: regional processing for the Bouguer gravity map. Therefore this method was employed here to help apprehension of regional tectonics and structures. The residual gravity map, shows gravity anomalies with a high gravity density value of 2.1mGal and a low gravity density value of -2.4mGal. The pink colour anomalies have density values ranging from 1.6mGal to 2.1mGal, which are prominent in the northwest and southeastern parts, with pockets in the southwestern part. The anomalies are trending in the northeast-southwest, northwest-southeast, east-west, and north-south directions. Figure 4 shows the residual gravity map of the Chad basin.

The upward continuation map indicates that the positive anomaly at the southeastern portion of the study area is deeper than the northwestern portion anomaly on the study area. The density range is between 27.4mGal and 30.7mGal (pink) on the map. The positive anomaly with weakly gravity signatures indicated at the central part of the map this could be from the weakly ferruginized ironstones.

To recognize the regional structure, the field was taken at 5000m (5km) plane of observation. This is to accentuate the consequence of deep sources and represses those of shallow sources like scattered local disturbances and noises. Therefore (Figure 5) shows the outcomes of the filtering processes. The result discloses a structural upliftment of high gravity field at the Northwest and eastern part of the map. The gravity effect is well conspicuous in the eastern region of the structures. This may be ascribed to the existence of the Migmatite gneiss complex in the crystalline basement rocks at the region. Furthermore, this may be explained as the mineral deposits either at significantly big scales or relatively near to the surface. In the same way, the blue-colored area at the middle part of the map specified the signature of low gravity.

The graphs of the logarithms of spectral energies against frequencies that were obtained for the various blocks are shown in Figure 6. Two linear segments were drawn from each graph. The depth to the centroid Z_0 of the gravity source from the slope of the longest part of the wave-length spectrum and the depth to the top boundary Z_t of that distribution from the slope of the second-longest wave length segment were calculated and varies from 3.55km to 7.50km and 1.08km to 2.07km respectively. Table 1 shows the summary of the depths Z_0 and Z_t which was used to compute the Curie point isotherm, geothermal gradient, and Heat flow.

The Curie-point isotherm map of the study area was acquired using equation 6. The calculated values are presented in Table 1. The Curie point value varies from 5.77km to 13.00km. These values were contoured to obtain the Curie point isotherm map. From the contoured map, the area was classified into two divisions. The areas with shallow Curie point depth with values varying from 5.2km to 6.2km covering the entire Northeaster part and the western boundary, while the area with deeper Curie point depth was observed central part of the study area with a value range from 9.2km to 10.6km Figure 9.

The Geothermal gradient map of the study area was obtained using equation 8. The calculated values (Table 1) were used to produce the contoured map. The vertical increase of temperature with depth in the area varies from $44.62^{\circ}\text{Ckm}^{-1}$ to $107.21^{\circ}\text{Ckm}^{-1}$. Two distinct groups of temperature increase with depth were observed on the contoured map. The first group with low-temperature increase with depth of $54.20^{\circ}\text{Ckm}^{-1}$ to $104.20^{\circ}\text{Ckm}^{-1}$, occurring in northwest, northeast, and southeast Figure 10.

The heat flow values vary from 111.55 to 268.03mWm⁻². An average heat flow density of 189.79mWm⁻² was computed for the Chad Basin. There is no distinct trend in the heat flow within the basin, although the values are relatively higher at the southwestern and northeastern axis of the basin (Figure 11). The heat flow contour in these two areas is closely packed.

Comparison of the Bouguer gravity anomaly, heat flow, and depth to the basement maps shows that the areas with high heat flows are associated with low negative gravity values (-55.5 to -26.4mGal). This may be connected with buried hills, the crest of folds, low sedimentary thickness, or depth to basement rocks. Therefore, those areas with low heat flow and very low gravity values are connected with high sedimentary thickness, graben, and trough of the undulating folds Figure 3.

The computed heat flow values in thebasin suggest that its sediments are thermally mature enough to generate hydrocarbons. In addition, gravity and depth to the basement map divulge adequate sediment thickness for formations in the basin. The fault-related structures recognize from seismic data have steep gradient planes which may not seal and can thus be multidirectional pathways for petroleum migration which finally disseminated in the formations. [26]in his research of the magnetic feature of the nearby Benue Trough noticed a magnetic anomaly on a dyke-like body. Therefore, such anomalies are finest accounted for to the greatest extent

by the presence of igneous intrusive bodies of varying depth and occurring inside the basement of sedimentary rocks. Moreover, these intrusive which must have extended to the Chad Basin have adverse effects on the preservation of petroleum within the basin.

5. Conclusion

In this research, gravity data has been used to investigate the presence of anomalies and the Curie point depth of the study area. The quantitative (Spectral analysis) interpretation technique was chosen to achieve the outlined objectives of this research. From Figure 9 the Curie point depths are deeper in the central, southwest, northwest, and eastern of the study area and shallower in the extreme northeast, southeast, and part of the Northwest. From Figure 10, the thermal gradient tends to be higher mainly in the northeast, northwest, and southeast of the study area and lower in most of the central part and southwest. From Figure 11, the heat flow tends to be higher mainly in the northeast and extreme southwest and southeastern part of the study area and lower in most of the central part and southwest. The above features of these regions according to [21], show that they might likely be sufficient sources for geothermal and thereby recommended for both geothermal exploration and exploitation.

6. Acknowledgments

The authors would like to thank the Department of Geophysics and measurement-control technology, East China University of Technology, Nanchang, Jiangxi Province, China for providing a convenient environment for this research to be carried out and to all the anonymous reviewers for their contributions towards the improvement of this manuscript.

References

- [1] Salem A, Ushijima K, Elsirafi A, Mizunaga H (2000) Spectral Analysis of Aeromagnetic data for Geothermal Reconnaissance of Quseir Area, Northern Red Sea Egypt. Proceedings World geothermal Congress Kyushu-Tohoku, Japan, 1669-1674.
- [2] DiPippio R (2005) Geothermal power plants: Principles, applications and case studies. Butterworth einemann: Elsevier, Oxford, England.
- [3] Blackwell D, Negraru P, Richards M (2006) Assessment of the enhance geothermal system resource base of the United States, Nat. Res. Res., 15(4):283-308
- [4] Tselentis GA (1991) An attempt to define curie depth in Greece from Aeromagnetic and heat flow data, PAGEOPH, 136(1):97-101.
- [5] Hisarlis ZM (1996) Determination of the Curie point depths in Western Anatolia and related with the Geothermal Areas, PhD Thesis, Istanbul University, Turkey.
- [6] Nurri DM, Timur UZ, Mumtaz H, Naci O (2005) Curie point depth variations to infer thermal structure of the crust at the African-Eurasian convergence zone, SW turkey, Journal of earth planets space, 57:373-383
- [7] Kingston DR, Dishroon CP, Williams PA (1983) Hydrocarbon playsand global basin classification. AAPG Bull 67(12):2194-2197
- [8] Carter JD, Barber W, Tait EA (1963) The Geology of parts of Adamawa, Bauchi and Bornu provinces in north eastern Nigeria. GeolSurv Nigeria Bull 30.
- [9] Okosun EA (2000) A preliminary assessment of the petroleum potentials from southwest Chad Basin (Nigeria). Borno J Geol 2(2):40-50.
- [10] Petters SW, Ekweozor CM (1982) Petroleum geology of Benue trough and south eastern Chad Basin Nigeria. AAPG Bull 66:1141-1149 6 J Petrol Explor Prod Technol (2012) 2:1-6
- [11] Genik GJ (1992) Regional framework structure and petroleum aspects of the rift basins in Niger, Chad and Central African Republic (C.A.R.). Tectonophysics 213:169-185
- [12] Okpikoro FE, Olorunniwo MA (2010) Seismic sequence architecture and structural analysis of North Eastern Nigeria Chad (Bornu) Basin. Cont J Earth Sci 5(2):1-9
- [13] Benkheilil J (1989) The origin and evolution of the Cretaceous Benue Trough, Nigeria. J Afr Earth Sci 8:251-282
- [14] Avbovbo AA, Ayoola EO, Osahon SA (1986) Depositional and structural styles in Chad Basin of Northeastern Nigeria. AAPG Bull 70(121):1787-1798
- [15] Udensi EE Interpretation of Total Magnetic Field over the Nupe Basin and the Surrounding Basement Complex, Using Aeromagnetic Data. Unpublished Ph.D. Thesis submitted to Ahmadu Bello University, Zaria. 2001.
- [16] Telford WM, Geldart LP, Sheriff RE (1990) Applied Geophysics (2nd Edition) Cambridge University Press.
- [17] Bhattacharyya BK, Leu LK Spectral analysis of gravity and magnetic anomalies due to two dimensional structures: Geophysics, 40(1975):993 - 10313
- [18] Okubo Y, Tanaka A, Matsubayashi O (1999) Curie point depth base on spectrum analysis of the magnetic anomaly data in east and Southeast Asia. Tectonophysics, 306:461 - 470
- [19] Stacey FD (1997) Physics of the earth. John Wiley and Sons, New York, 414
- [20] Nwanko LI (2007) Spectral evaluation of aeromagnetic anomaly map for geothermal exploration in part of Nupe basin, West central Nigeria. Ph.D Thesis University of Ilorin.
- [21] Tanaka A, Okubo Y, Matsubayashi O (1999) Curie point depth base on spectrum analysis of the magnetic anomaly data in east and Southeast Asia. Tectonophysics, 306:461 - 470
- [22] Stampolidis A, Kane I, Tsokas GN, Tsourlo P (2005) Curie point depths of Albania inferred from ground total magnetic data. Surveys in Geophysics, 26:461 - 481
- [23] Popoola OI, Ojo AE (2010) Effects of poor conductor on continental crust heat flow parameters. Pacific journal of science and Technology, 11(1): 483-501
- [24] Abdulsalam NN, Nasir MA, Likason, KO (2011) Identification of Linear Features Using Continuation Filters over Koton Karfi Area from Aeromagnetic Data. World Rural Observation, 3(1):1-8

- [25] Kennedy WQ (1964) The structural differentiation of Africa in the Panafrican 500 Ma tectonic episode. In; 8th Ann. Rep. Res. Inst. Afr. Géol. Leeds University, U.K, 48-49
- [26] Ofoegbu CO (1985) Interpretation of a linear magnetic feature near Mutum-Biyu, Nigeria. *Revista Brasileira de Geofísica* 3:91–97

Author Profile



Sulaiman Garba Yana received B.Sc. in Physics from University of Abuja, Nigeria in the year 2008. After his one year compulsory youth service, He joined Ajaokuta steel company limited, under federal ministry of mines and steel. He received M.Sc. in Geophysics from East China University of Technology, Nanchang, China in the year 2018. He is presently a PhD student in Geophysics at East China University of Technology, Nanchang, Jiangxi Province, China.